Transport in Porous Media **12:** 19–29, 1993.

Natural Convection in a Horizontal Porous Layer with Anisotropic Thermal Diffusivity

LEIV STORESLETTEN
Department of Mathematics, Agder College, Kristiansand, Norway

(Received: 9 August 1991)

Abstract. The present paper is concerned with free convection in a horizontal porous layer with anisotropic thermal diffusivity. It is assumed that the diffusivity has rotational symmetry, with a symmetry axis making an arbitrary angle against the vertical. The critical Rayleigh number and wave number at marginal stability are calculated and the steady motion occurring at convection onset is examined. It is found that there are two different types of convection cells, depending on whether the longitudinal diffusivity is larger than the transverse diffusivity or not. In the former case, the convection cells are rectangular with vertical lateral walls. In the latter case, however, the lateral cell walls are tilted as well as curved.

Key words. Anisotropy, thermal diffusivity, marginal stability, flow pattern, porous layer, convection.

1. Introduction

Convective flows in porous media are of interest in many varied problems in geophysics and energy-related systems, like geothermal energy systems, oil reservoir modelling, open-pore insulating systems, and diagenetic processes in sedimentary basins, to name but a few.

Natural convection in *anisotropic* porous media has attracted the interest of several researchers over the last 15 years. In the middle of the seventies, it was shown that anisotropy in the mechanical and thermal properties effects the marginal stability condition as well as the preferred width of the convection cells (Castinel and Combarnous, 1974; Epherre 1975). On the other hand, Kvernvold and Tyvand (1979) showed that even a three-dimensional anisotropy does not lead to any new mathematical difficulties or essential new flow patterns at convention onset compared with isotropy. This is true only as long as one of the principal axes of the anisotropic medium is vertical. This requirement has been maintained in almost all former work in the field, see the review article by McKibbin (1984) as well as McKibbin (1986) and Nilsen and Storesletten (1990). Tyvand and Storesletten (1991) seem to have been the first to have studied natural convection in an anisotropic porous medium where none of the principal axes is vertical. They considered a horizontal porous layer with anisotropy in the permeability, whereas the thermal diffusivity was isotropic. This was sufficient to achieve qualitatively new flow patterns with tilted plane of motion or tilted lateral cell walls. In the present work,

we study the analogous problem for a layer with anisotropy in the thermal properties.

We consider natural convection in a horizontal fluid-saturated porous layer with anisotropic thermal diffusivity. For simplicity, it is assumed that the diffusivity has rotational symmetry with a symmetry axis making an arbitrary angle against the vertical. The direction of the symmetry axis is denoted longitudinal, which means that the diffusivity is transversely isotropic. Moreover, our analysis is restricted to full isotropy in the permeability. The critical Rayleigh number and wave number at marginal stability are calculated and the steady motion occurring at the onset of convection is examined. It is found that there exist two different types of convection cells (rolls), depending on whether the longitudinal diffusivity is larger than the transverse diffusivity or not. In the former case, the convection cells are rectangular with vertical lateral walls, whereas the lateral cell walls are tilted as well as curved in the latter case.

These results correspond mainly to those found in the analogous problem with anisotropic permeability, studied by Tyvand and Storesletten (1991). On the other hand, there are also a few essential differences, which are discussed in Section 3.

2. Mathematical Formulation

We consider free convection in a fluid-saturated porous layer with anisotropic thermal diffusivity. The layer is bounded above and below by two infinite and impermeable heat-conducting horizontal planes. The upper and lower boundaries are separated by a distance h and are at constant temperatures T_0 and $T_0 + \Delta T$, respectively. Here the characteristic temperature difference ΔT is positive, which means that the layer is heated from below.

It is assumed that the thermal diffusivity has rotational symmetry with a symmetry axis making an arbitrary angle against the vertical. The direction of the symmetry axis is denoted longitudinal, which means that the diffusivity is transversely isotropic. Let κ_L and κ_T be the longitudinal and transverse components of the diffusivity tensor $\mathbf{D}^*$, i.e.

$$\mathbf{D}^* = \kappa_L \mathbf{i}'\mathbf{i}' + \kappa_T(\mathbf{j}'\mathbf{j}' + \mathbf{k}'\mathbf{k}') \tag{1}$$

where $\mathbf{i}'$, $\mathbf{j}'$ and $\mathbf{k}'$ are unit vectors along the principal axes. A Cartesian frame of reference is chosen, with x- and y-axis at the lower boundary, where the x-axis is aligned along the horizontal projection of $\mathbf{i}'$. The z-axis is directed opposite to gravity. The unit vectors in the x, y, and z directions are denoted $\mathbf{i}$, $\mathbf{j}$, and $\mathbf{k}$. By introducing the anisotropy parameter

$$\eta = \frac{\kappa_T}{\kappa_L}, \tag{2}$$

the dimensionless diffusivity tensor $\mathbf{D} = D^*/\kappa_T$ may be written as

$$\begin{aligned}\mathbf{D} &= \eta^{-1}\mathbf{i}'\mathbf{i}' + \mathbf{j}'\mathbf{j}' + \mathbf{k}'\mathbf{k}' \\ &= D_{11}\mathbf{ii} + \mathbf{jj} + D_{13}(\mathbf{ik} + \mathbf{ki}) + D_{33}\mathbf{kk}\end{aligned} \tag{3}$$

Here

$$\begin{aligned}&D_{11} = \eta^{-1}\cos^2\beta + \sin^2\beta, \qquad D_{13} = (\eta^{-1} - 1)\cos\beta\sin\beta, \\ &D_{33} = \cos^2\beta + \eta^{-1}\sin^2\beta\end{aligned} \tag{4}$$

and β is the angle between the longitudinal and horizontal direction, i.e. the angle determined by $\mathbf{i}'$ and $\mathbf{i}$.

The linearized version of the governing equations in dimensionless form may be written (Kvernvold and Tyvand, 1979)

$$\mathbf{v} + \nabla p - \mathrm{Ra}\,\theta\mathbf{k} = 0, \tag{5}$$

$$\nabla\cdot\mathbf{v} = 0, \tag{6}$$

$$\frac{\partial\theta}{\partial t} - w = \nabla\cdot(D\cdot\nabla\theta) \tag{7}$$

Here Darcy law and the Boussinesq approximation have been used and the density is assumed to be a linear function of the temperature. Moreover, $\mathbf{v} = u\mathbf{i} + v\mathbf{j} + w\mathbf{k}$ is the velocity, p the pressure, t the time, and θ is the deviation from the linear temperature distribution corresponding to the motionless conduction state. Ra is the Rayleigh number defined by

$$\mathrm{Ra} = \frac{Kg\gamma\,\Delta T h}{\kappa_T \nu}, \tag{8}$$

where K is the permeability, g the acceleration due to gravity, γ the thermal expansion coefficient, and ν the kinematic viscosity of the saturating fluid.

Equation (7) may be written

$$\frac{\partial\theta}{\partial t} - w = D_{11}\frac{\partial^2\theta}{\partial x^2} + \frac{\partial^2\theta}{\partial y^2} + D_{33}\frac{\partial^2\theta}{\partial z^2} + 2D_{13}\frac{\partial^2\theta}{\partial x\,\partial z}. \tag{9}$$

Applying the operator

$$\left(\frac{\partial^2}{\partial x\,\partial z}, \frac{\partial^2}{\partial y\,\partial z}, -\nabla_1^2\right)$$

to Equation (5), adding the component equations, and using the continuity Equation (6), we get the equation

$$\nabla^2 w = \mathrm{Ra}\,\nabla_1^2\theta, \tag{10}$$

where

$$\nabla_1^2 = \frac{\partial^2}{\partial x^2} + \frac{\partial^2}{\partial y^2}. \tag{11}$$

The operator $\mathrm{Ra}\,\nabla_1^2$ applied to Equation (9), substituting Equation (10), finally gives the equation

$$\nabla^2\left[\frac{\partial w}{\partial t} - D_{11}\frac{\partial^2 w}{\partial x^2} - \frac{\partial^2 w}{\partial y^2} - D_{33}\frac{\partial^2 w}{\partial z^2} - 2D_{13}\frac{\partial^2 w}{\partial x\,\partial z}\right]$$

$$= \mathrm{Ra}\left[\frac{\partial^2 w}{\partial x^2} + \frac{\partial^2 w}{\partial y^2}\right]. \tag{12}$$

Impermeable and perfectly heat-conducting boundaries require that

$$w = \theta = 0 \quad \text{at} \quad z = 0 \quad \text{and} \quad z = 1. \tag{13}$$

By using Equation (10), these boundary conditions are expressed by vertical velocity alone:

$$w = \frac{\partial^2 w}{\partial z^2} = 0 \quad \text{at} \quad z = 0 \quad \text{and} \quad z = 1. \tag{14}$$

3. Marginal Stability and Steady Convection Cells

At the onset of convection, the preferred flow cells tend to arrange themselves such that the tangential diffusivity along the streamlines is as small as possible. Let us first consider the case $\beta = 0$. When $\eta < 1$, we have minimum diffusivity in directions orthogonal to the x-axis. This indicates that the preferred motion is independent of x. When $\eta > 1$, it is clear that motion in the y-direction should be avoided, as the diffusivity is maximum in that direction. Thus, it is reasonable to expect convective motion in the (x, y)-plane, independent of y.

In the case $\beta = 0$, these physical arguments suggest that the preferred motion at the onset of convection is independent of x or y depending, respectively, on whether $\eta < 1$ or $\eta > 1$. This situation turns out to be valid for arbitrary values of β, i.e. $0 \leqslant \beta < \pi$. In Appendix A, these hypothesis are numerically confirmed by showing that the Rayleigh number in both cases is a local minimum.

Case I: $\eta < 1$. In this case, β denotes the angle between the x-axis and the direction with maximum thermal diffusivity. Since the solutions are independent of x, it is easy to solve the problem analytically. The curl of Equation (5) gives

$$\frac{\partial u}{\partial y} = \frac{\partial u}{\partial z} = 0, \tag{15}$$

which indicates that u is a constant, here given the value zero. It follows that the motion at convection onset is two-dimensional. The convection cells are rectangular with vertical planes of motion. At this point, there is an essential difference between the present case and the analogous case for a porous layer with anisotropic permeability, where the planes of motion were tilted (Tyvand and Storesletten, 1991). This tilt was purely mechanical determined, decoupled from any thermal effects.

In the absence of x-dependence the governing Equation (12) reduces to

$$\left(\frac{\partial^2}{\partial y^2}+\frac{\partial^2}{\partial z^2}\right)\left[\frac{\partial w}{\partial t}-\frac{\partial^2 w}{\partial y^2}-D_{33}\frac{\partial^2 w}{\partial z^2}\right]=\mathrm{Ra}\frac{\partial^2 w}{\partial y^2}. \tag{16}$$

The preferred mode of disturbance which satisfies the boundary conditions is given by

$$w=\sin(\pi z)\exp(imy+\sigma t), \tag{17}$$

where m is a wave number, σ is the growth rate, and i is the imaginary unit. It is shown in Appendix B that the principle of exchange of stabilities is valid, i.e. σ is real and marginal stability is defined by $\sigma=0$. Substituting solution (17) into Equation (16), we find the Rayleigh number at onset of convection to be

$$\mathrm{Ra}=(1+\pi^2/m^2)(m^2+D_{33}\pi^2). \tag{18}$$

Minimizing Ra with respect to m, we obtain the critical Rayleigh number

$$\mathrm{Ra}_c=\pi^2(1+\{\cos^2\beta+\eta^{-1}\sin^2\beta\}^{1/2})^2. \tag{19}$$

The corresponding critical wave number is

$$m_c=\pi(\cos^2\beta+\eta^{-1}\sin^2\beta)^{1/4}. \tag{20}$$

From Equation (19), it follows that $\mathrm{Ra}_c\to 4\pi^2$ as $\eta\to 1$. For η fixed, Ra_c obtains its minimum $4\pi^2$ for $\beta=0$ and its maximum $\pi^2(1+1/\sqrt{\eta})^2$ for $\beta=\pi/2$. For these two values of β, the results coincide with those found by Kvernvold and Tyvand (1979).

Case II: $\eta>1$. In this case β denotes the angle between the x-axis and the direction with minimal thermal diffusivity. When $\eta>1$, it turns out that the solutions are independent of y. In order to demonstrate this numerically (see Appendix A), we also include solutions dependent on y, i.e. we consider solutions of the general form

$$w=Z(z)\exp(i(kx+my)+\sigma t), \tag{21}$$

where k and m are wave numbers and the amplitude Z has to satisfy the boundary conditions (14), which imply

$$Z(0)=Z''(0)=Z(1)=Z''(1)=0. \tag{22}$$

The solution (21) substituted into Equation (12) leads to a fourth-order linear differential equation for Z with constants coefficients. Its general solution is

$$Z(z)=A_1\exp(r_1 z)+A_2\exp(r_2 z)+A_3\exp(r_3 z)+A_4\exp(r_4 z), \tag{23}$$

where r_1, r_2, r_3, and r_4 are roots of the polynomial equation

$$(k^2 + m^2 - r^2)(\sigma + D_{11}k^2 + m^2 - D_{33}r^2 - 2D_{13}ikr) = \mathrm{Ra}(k^2 + m^2). \tag{24}$$

The constants A_1, A_2, A_3, and A_4 have to satisfy the boundary conditions (22), which leads to a linear homogeneous system of algebraic equations. Nontrivial solutions imply that the determinant of the coefficient matrix is zero:

$$\begin{vmatrix} 1 & 1 & 1 & 1 \\ r_1^2 & r_2^2 & r_3^2 & r_4^2 \\ \exp(r_1) & \exp(r_2) & \exp(r_3) & \exp(r_4) \\ r_1^2\exp(r_1) & r_2^2\exp(r_2) & r_3^2\exp(r_3) & r_4^2\exp(r_4) \end{vmatrix} = 0. \tag{25}$$

As in Case I ($\eta < 1$), it follows from Appendix B that the growth rate $\sigma = 0$ at marginal stability. Thus, in order to find the critical Rayleigh number Ra_c, we put $\sigma = 0$ in Equation (24). Given the parameters η, β and the wave numbers k, m, Equations (24) and (25) represent an eigenvalue problem, the eigenvalues being the Rayleigh numbers $R_0 < R_1 < R_2 < \ldots$ where the critical Rayleigh number is

$$\mathrm{Ra}_c = \min R_0(\eta, \beta, k, m), \quad k \geqslant 0, m \geqslant 0. \tag{26}$$

The eigenvalue problem (24) and (25) (with $\sigma = 0$) is solved numerically. It turns out that Ra_c is obtained at $m = 0$ which means that the steady solutions at convection onset are independent of y. This fact is demonstrated numerically in the Appendix A.

In Figure 1 we present marginal stability curves, displaying the Rayleigh number Ra as a function of the wave number k. The curves are computed for the value $\eta = 2$, for the cases $\beta = 17.5°$, $35°$, $52.5°$, and $70°$, respectively.

Table I shows the computed values of Ra_c for various values of the anisotropy ratio η and the angle β. For moderate values of η, less than 2 for instance, the critical Rayleigh number depends very weakly on the angle β. For larger values of η there is a stronger dependence, see Table I.

For given η, the critical Rayleigh numbers are equal for the cases $\beta = 0°$ and $\beta = 90°$, which is known from Kvernvold and Tyvand (1979). Moreover, Ra_c depends on the angle β, and for each η there exists an angle β_m giving a minimal critical Rayleigh number R_m. Table II shows β_m, R_m and the corresponding wave number k_m. We observe that $\beta_m \to 45°$ as $\eta \to 1$ ($\eta < 1$).

It turns out that the computed Tables I and II in the present problem have a close relationship to the corresponding tables in the analogous problem with anisotropic permeability (Tyvand and Storesletten, 1991). In Case II, the tables are in fact identical if η and β are replaced by $1/\xi$ and $(\pi/2 - \beta)$ in the analogous problem. This fact is easily deduced from the governing equations. Putting $\sigma = m = 0$ and applying the above-mentioned transformation, the polynomial Equation (24) becomes identical with the corresponding Equation (26) in Tyvand and Storesletten (1991).

Concerning the convection cells there exists no such close relationship between the two problems. The plane of motion is vertical and the lateral cell walls are tilted as

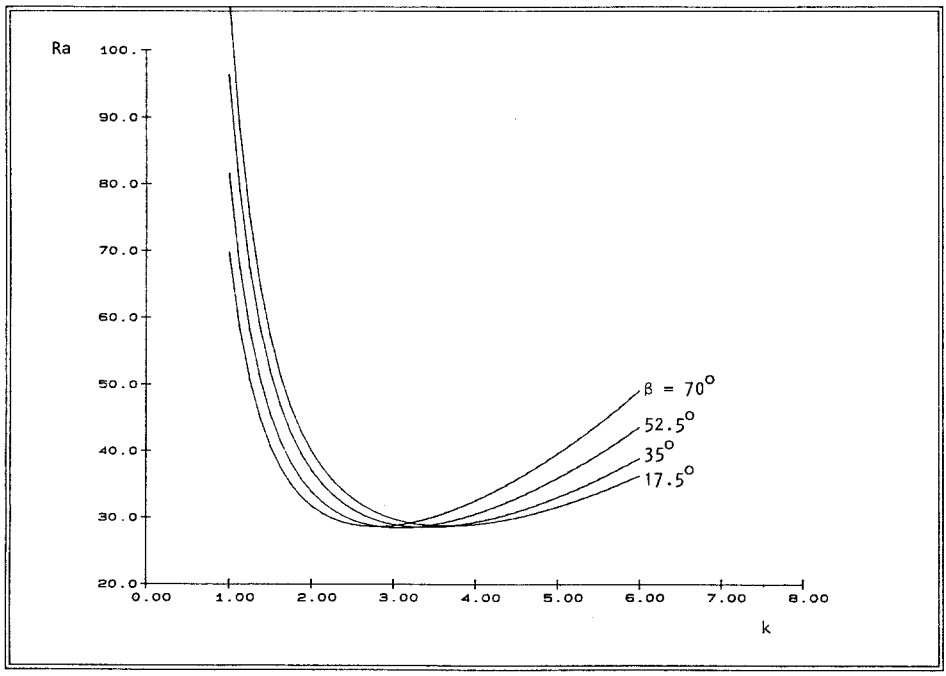

Fig. 1. Marginal stability curves when $\eta = 2$ for the cases $\beta = 17.5°$, 35°, 52.5° and 70°.

well as curved also in the present problem. However, the tilt is opposite directed and caused by purely thermal effects.

The computed streamlines are displayed in Figure 2 at $\beta = 40.1°$ for the cases $\eta = 1.00$, 2.00, 4.00, and 8.00. A stream function has been defined in order to construct these curves. There is a constant increment in the stream function between two neighbouring streamlines.

The lateral cell walls have no tilt at the stagnation points at the top and bottom of the layer, whereas the maximum tilt is found in the middle of the layer, i.e. at $z = 1/2$.

Table I. The computed values of Ra_c for various values of η and β

β/η	1.143	1.333	1.60	2.00	2.667	4.00	8.00
0°	36.970	34.367	31.643	28.762	25.658	22.207	18.082
10°	36.968	34.358	31.625	28.730	25.609	22.173	17.994
20°	36.963	34.337	31.577	28.643	25.472	21.940	17.737
30°	36.957	34.312	31.516	28.529	25.282	21.653	17.335
40°	36.952	34.292	31.466	28.427	25.100	21.346	16.848
50°	36.952	34.289	31.452	28.385	25.000	21.131	16.401
60°	36.956	34.303	31.483	28.434	25.053	21.143	16.215
70°	36.962	34.330	31.548	28.561	25.268	21.463	16.571
80°	36.968	34.356	31.615	28.701	25.535	21.955	17.489
90°	36.970	34.367	31.643	28.762	25.658	22.207	18.082

Table II. The computed values of β_m, k_m, and R_m for various values of η.

η	1.010	1.143	1.333	1.600	2.000	2.667	4.000	8.000
β_m	45.1°	46.0°	46.6°	48.6°	50.1°	51.9°	54.7°	59.3°
k_m	3.1416	3.13	3.14	3.12	3.10	3.07	3.00	2.83
R_m	39.2826	36.952	34.288	31.451	28.385	24.977	21.101	16.214

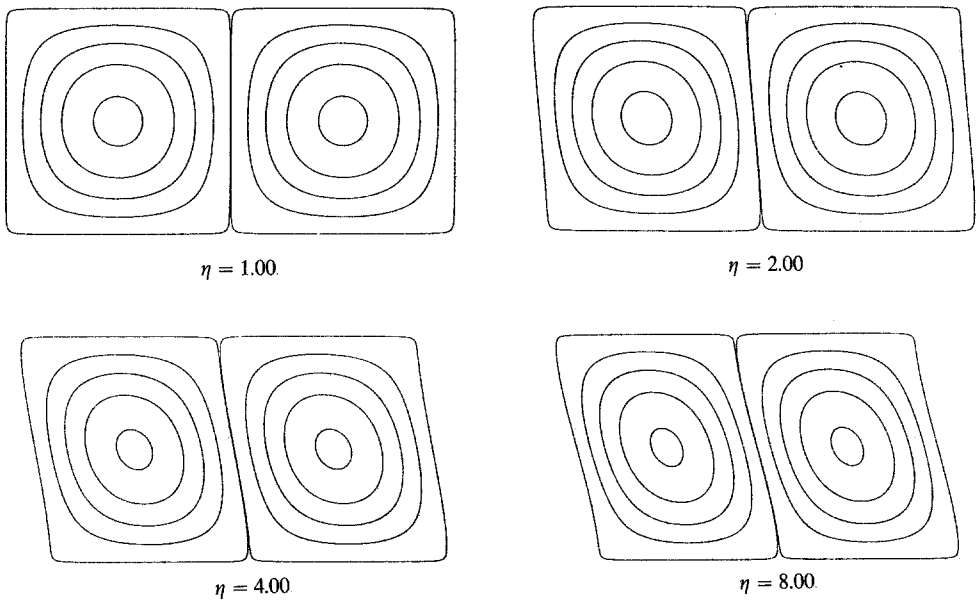

Fig. 2. Computed streamlines at $\beta = 40.1°$ for the cases $\eta = 1.00$, 2.00, 4.00, and 8.00.

4. Summary

We have considered natural convection in a horizontal porous layer with anisotropy in the thermal diffusivity. It is assumed that the diffusivity has rotational symmetry with a symmetry axis making an angle $(90° - \beta)$ against the vertical direction. The direction of the symmetry axis is denoted as longitudinal, which means that the diffusivity is transversely isotropic.

We have examined the linear stability and the steady flow patterns at the onset of convection. Two different types of convection cells (rolls) were found, both two-dimensional: If the longitudinal diffusivity is larger than the transverse $(0 < \eta < 1)$, the convection cells are rectangular with vertical lateral cell walls like the isotropic case. For the converse case $(\eta > 1)$, the plane of motion is vertical whereas the lateral cell walls are tilted as well as curved. The preference for these different flow patterns is explained as a preference for flow directions with as small a tangential diffusivity along the streamlines as possible.

In Case I, $0 < \eta < 1$, the problem is solved analytically. The critical Rayleigh number is found to be

$$\mathrm{Ra}_c = \pi^2(1 + \{\cos^2\beta + \eta^{-1}\sin^2\beta\}^{1/2})^2.$$

For given η, Ra_c attains its minimum $4\pi^2$ for $\beta = 0$ and its maximum $\pi^2(1 + 1/\sqrt{\eta})^2$ for $\beta = \pi/2$. Here β denotes the angle between the horizontal and longitudinal direction.

In Case II, $\eta > 1$, the critical Rayleigh number has to be determined numerically, see Table I. For given η, the number Ra_c attains its maximum for $\beta = 0$ and $\beta = \pi/2$. The minimum values R_m depending on β are calculated in Table II. The computed streamlines are shown in Figure 2.

Appendix A

For physical reasons, given in Section 3, it is expected that the solutions at the onset of convection are independent of x ($k = 0$) or y ($m = 0$) depending on whether $\eta < 1$ or $\eta > 1$. These conjectures are confirmed numerically by showing that the Rayleigh number for marginal stability attains a local minimum for $k = 0$ when $\eta < 1$, and for $m = 0$ when $\eta > 1$. We have tested the hypothesis for various values of η and β. The results are given in the tables on page 28, for $\eta = 0.25$, 0.50, 2.00, and 4.00 for the angle $\beta = 30°$. From these tables we note that the Rayleigh number at marginal stability is not always a local minimum when the wave number is sufficiently far from its preferred value.

Appendix B: A Proof of the Principle of Exchange of Stabilities (im (σ) = 0)

We shall now show that the principle of exchange of stabilities is valid for the boundary value problem (5), (6), (7), and (13), i.e. the growth rate σ is real and the marginal stability is defined by $\sigma = 0$.

Multiplying Equations (5) and (7) by $\mathbf{v}^*$ and $\mathrm{Ra}\,\theta^*$ (* denotes the complex conjugate), respectively, and adding the equations, we get

$$\sigma\,\mathrm{Ra}\,\theta\theta^* = \mathrm{Ra}(w\theta^* + w^*\theta) - \mathbf{v}^*\cdot\mathbf{v} - \mathbf{v}^*\cdot\nabla p + \\ + \mathrm{Ra}\left(D_{11}\frac{\partial^2\boldsymbol{\theta}}{\partial x^2} + \frac{\partial^2\boldsymbol{\theta}}{\partial y^2} + D_{33}\frac{\partial^2\boldsymbol{\theta}}{\partial z^2} + 2D_{13}\frac{\partial^2\boldsymbol{\theta}}{\partial x\,\partial z}\right) \tag{B1}$$

Here $\partial\boldsymbol{\theta}/\partial t$ is replaced by $\sigma\theta$, where σ is a constant which can be complex.

Assuming solutions periodic in x and y, we introduce the following notation

$$\langle(\ )\rangle = 1/\mathrm{Ra}\int_0^1\int_{y_0}^{y_1}\int_{x_0}^{x_1}(\ )\,\mathrm{d}x\,\mathrm{d}y\,\mathrm{d}z,$$

where $(x_1 - x_0)$ and $(y_1 - y_0)$ are the periods in the x- and y-directions, respectively.

The case $\eta = 0.25$ and $\beta = 30°$:

	k=0.00	k=0.01	k=0.10
m=2.7	Ra=57.244859	Ra=57.245007	Ra=57.259714
m=3.00	Ra=55.082069	Ra=55.082274	Ra=55.102637
m=3.25	Ra=53.842696	Ra=53.842936	Ra=53.866668
m=3.50	Ra=53.306997	Ra=53.307257	Ra=53.333021
m=3.75	Ra=53.325932	Ra=53.326205	Ra=53.353197
m=4.00	Ra=53.795531	Ra=53.795811	Ra=53.823536
m=4.25	Ra=54.641471	Ra=54.641755	Ra=54.669902
m=4.50	Ra=55.809482	Ra=55.809768	Ra=55.838140
m=4.75	Ra=57.259188	Ra=57.259475	Ra=57.287948

The case $\eta = 0.50$ and $\beta = 30°$:

	k=0.00	k=0.01	k=0.10
m=2.50	Ra=47.938428	Ra=47.938380	Ra=47.933689
m=2.75	Ra=45.869786	Ra=45.869820	Ra=45.873194
m=3.00	Ra=44.735650	Ra=44.735734	Ra=44.744004
m=3.25	Ra=44.296813	Ra=44.296927	Ra=44.308267
m=3.50	Ra=44.396313	Ra=44.396448	Ra=44.409762
m=3.75	Ra=44.927696	Ra=44.927843	Ra=44.942454
m=4.00	Ra=45.816695	Ra=45.816851	Ra=45.832326
m=4.25	Ra=47.010223	Ra=47.010386	Ra=47.026442
m=4.50	Ra=48.469517	Ra=48.469683	Ra=48.486133

The case $\eta = 2$ and $\beta = 30°$:

	m=0.00	m=0.01	m=0.10
k=2.50	Ra=31.681117	Ra=31.681065	Ra=31.675987
k=2.75	Ra=30.085635	Ra=30.085641	Ra=30.086267
k=3.00	Ra=29.130747	Ra=29.130788	Ra=29.134885
k=3.25	Ra=28.649077	Ra=28.649141	Ra=28.655420
k=3.50	Ra=28.530817	Ra=28.530895	Ra=28.538583
k=3.75	Ra=28.701502	Ra=28.701589	Ra=28.710205
k=4.00	Ra=29.109190	Ra=29.109283	Ra=29.118520
k=4.25	Ra=29.716757	Ra=29.716855	Ra=29.726511
k=4.50	Ra=30.497097	Ra=30.497198	Ra=30.507141

The case $\eta = 4$ and $\beta = 30°$:

	m=0.00	m=0.01	m=0.10
k=3.00	Ra=23.135779	Ra=23.135858	Ra=23.143594
k=3.25	Ra=22.364496	Ra=22.364590	Ra=22.373917
k=3.50	Ra=21.904812	Ra=21.904916	Ra=21.915205
k=3.75	Ra=21.687596	Ra=21.687706	Ra=21.698580
k=4.00	Ra=21.664629	Ra=21.664743	Ra=21.675970
k=4.25	Ra=21.801453	Ra=21.801569	Ra=21.813001
k=4.50	Ra=22.072908	Ra=22.073025	Ra=22.084570
k=4.75	Ra=22.460281	Ra=22.460398	Ra=22.471996
k=5.00	Ra=22.949416	Ra=22.949533	Ra=22.961145

Integration of Equation (B1) over the fluid volume $(x_0, x_1)x(y_0, y_1)x(0, 1)$, application of Equations (6) and (13), and partial integration, finally produces the equation

$$\sigma\langle\theta\theta^*\rangle = \langle w\theta^* + w^*\theta\rangle - (1/\mathrm{Ra})\langle \mathbf{v}^* \cdot \mathbf{v}\rangle -$$

$$- \left\langle D_{11}\frac{\partial\theta}{\partial x}\frac{\partial\theta^*}{\partial x} + \frac{\partial\theta}{\partial y}\frac{\partial\theta^*}{\partial y} + D_{33}\frac{\partial\theta}{\partial z}\frac{\partial\theta^*}{\partial z}\right\rangle -$$

$$- D_{13}\left\langle \frac{\partial\theta}{\partial x}\frac{\partial\theta^*}{\partial z} + \frac{\partial\theta^*}{\partial x}\frac{\partial\theta}{\partial z}\right\rangle. \tag{B2}$$

Since all terms at the right-hand side are real, it follows that $\mathrm{im}(\sigma) = 0$.

Acknowledgements

The author is grateful to Dr Peder A. Tyvand, Agricultural University of Norway, for having directed his attention to the problem investigated in this paper. He also wishes to thank his colleague Dr Åsvald Lima for helpful instruction in connection with the computing and the graphics, and Professor Enok Palm for helpful discussions.

References

Castinel, G. and Combarnous, M., 1974, Critère d'apparition de la convection naturelle dans une couche poreuse anisotrope horizontale, *C.R. Acad. Sci. Ser. B* **287**, 701–704.

Epherre, J. F., 1975, Critère d'apparition de la convection naturelle dans une couche poreuse anisotrope, *Rev. Thermique* **168**, 949–950.

Kvernvold, O. and Tyvand, P. A., 1979, Nonlinear thermal convection in anisotropic porous media, *J. Fluid Mech.* **90**, 609–624.

McKibbin, R., 1984, Thermal convection in layered and anisotropic porous media: A review, in R. A. Wooding and I. White (eds), *Convective Flows in Porous Media*, DSIR, Wellington, New Zealand, pp. 113–127.

McKibbin, R., 1986, Thermal convection in a porous layer: Effects of anisotropy and surface boundary conditions, *Transport in Porous Media* **1**, 271–292.

Nilsen, T. and Storesletten, L., 1990, An analytical study on natural convection in isotropic and anisotropic porous channels, *Trans. ASME C: J. Heat Transfer* **112**, 396–401.

Tyvand, P. A. and Storesletten, L., 1991, Onset of convection in an anisotropic porous medium with oblique principal axes, *J. Fluid Mech.* **226**, 371–382.